

The Quark Model of the Electron and the Vacuum Pion Tetrahedron Fabric

Rami Rom^(a)

Abstract: We propose a quark model for the electron and the vacuum pion tetrahedron fabric, where the electron is a non-elementary, non-point like exotic tetraquark, and the vacuum fabric is comprised of exotic pion tetraquark tetrahedrons comprised of the u , d , \tilde{u} , \tilde{d} quarks and antiquarks. We assume that electron tetraquarks perform rapid quark flavor exchange reactions with the vacuum pion tetraquark tetrahedrons fabric forming an electron and pion tetraquarks cloud. Motion of the electron tetraquark tetrahedron on the vacuum pion tetraquark tetrahedron fabric is performed by a u and d quark flavor exchange reactions by tunneling through a potential barrier between the electron tetraquark tetrahedron and the vacuum pion tetraquark tetrahedron sites that transform the electron tetraquark tetrahedrons into pion tetraquark tetrahedrons and vice versa. We develop a semiclassical quark molecular dynamics scheme for bound states of mesons and exotic tetraquarks and show that the exotic pion tetraquark tetrahedron binding energy is about 0.0486 GeV comparing to the free di-meson $d\tilde{d}$ and $u\tilde{u}$ energies. Lattice QCD computations may prove the quark model for the electron and the vacuum pion tetraquark fabric and may allow calculating the mass of the proposed pion and electron exotic tetraquarks.

Keywords: Antimatter, Quantum vacuum, Lattice QCD and Exotic tetraquarks.

(a) Email: romrami@gmail.com

1. Problems with the Quantum Theory of the Electron

(a) Schrödinger's electron wavepacket width grows linearly with time in free space - Erwin

Schrödinger introduced the idea of a particle wave packet and the superposition of eigenfunctions and found that a gaussian wavepacket remains compact for a quantum harmonic oscillator¹. However, Schrödinger found that in free space the width of the gaussian wavepacket grows linearly with time. If an electron wavepacket is initially localized in a region of an atomic dimension of 10^{-10} meters, the width of the wavepacket doubles in about 10^{-16} seconds and after about a milli-second the wave packet width grows to about a kilometer².

(b) Dirac's negative energy states make the electron positive energy states unstable – Paul

Dirac proposed a relativistic wave equation and found a new set of negative energy antimatter states³. Dirac thought that since the positive energy electron solutions would decay to the negative energy states there must be an infinite number of invisible electrons that occupy the negative states and prevent the electron decay based on Pauli exclusion principle⁴.

(c) The standard model of particle physics assumes that the electron is an elementary point-

like particle with infinite mass and charge densities - Dirac assumed that electrons are not point like particles and proposed a spherical shell electron model⁵.

(d) Feynman's integrals for the electron self-energy and the vacuum polarization diverge -

Robert Oppenheimer showed that the vacuum polarization and the electron self-energy are not small perturbative corrections that diverge. Paul Dirac and Richard Feynman did not like the renormalization scheme that succeeded to cancel these infinities. Dirac thought that electrons interact strongly with the vacuum electron-positron virtual pairs and hence are never bare in contrast to Feynman's diagrams, where bare electrons propagate in free

space in zero-order⁶⁻⁷. Dirac thought that better understanding of the vacuum structure is needed for the quantum electron theory⁸.

2. The Addressed Questions

The questions we address in this paper are:

1. Are electrons non-elementary, non-point like particles comprised of exotic tetraquarks?
2. Is the quantum vacuum filled with pion tetraquark tetrahedrons fabric?
3. Does electron motion in the vacuum occurs via rapid u and d quark flavor exchanges, and a \tilde{u} and \tilde{d} antiquark flavor exchanges in a second electron tetraquark state?

3. The Quantum Vacuum Exotic Pion Tetraquark Fabric

We assume that the quantum vacuum is filled with exotic pion tetraquark tetrahedrons particles that form the vacuum fabric⁹⁻¹³. We note that the vacuum pion tetraquark tetrahedrons are not ordinary particles since they are composed of 50% antiquarks and 50% quarks. We assume that the quarks and antiquarks do not annihilate each other, and that their dynamics may be modeled with quark molecular dynamics with a quark exchange operation described below. We assume that in each site in the vacuum fabric there is a single exotic tetraquark particle, $u\tilde{d}d\tilde{u}$, composed of the two light quarks, d and u , and their antiquark pairs, \tilde{d} and \tilde{u} . We first develop the quark molecular dynamics scheme for bound mesons and pion tetraquark tetrahedron systems and then continue to the electron and vacuum pion tetraquark tetrahedron system using the semiclassical quark molecular dynamics and a quantum mechanical computation scheme.

A. The Bound Meson Molecular Dynamics

The quark and antiquark interaction with the quark exchange operations defined below create bound periodic trajectories where quarks and the antiquarks follow mirrored paths. For the $d\tilde{d}$ meson semiclassical quark molecular dynamics, we use a pair potential with a string tension $\sigma = 1 \text{ GeV/femtometer}$ ¹⁴.

$$V_{d,\bar{d}}(r_{1,2}) = -\frac{1}{9} \frac{e^2}{4\pi \epsilon_0 r_{1,2}} + \sigma r_{1,2} \quad (1a)$$

The d and \bar{d} quarks equations of motion are derived from the Hamiltonian below and solved numerically with Runge Kutta 4 ODE scheme.

$$H_{d,\bar{d}}(v_d, v_{\bar{d}}, r_{1,2}) = \frac{1}{2} m_d v_d^2 + \frac{1}{2} m_{\bar{d}} v_{\bar{d}}^2 + V_{d,\bar{d}}(r_{1,2}) \quad (1b)$$

$$\dot{v}_{x1(d)} = -\frac{1}{m_d} \frac{dV_{d,\bar{d}}(r_{1,2})}{dx_1}, \quad \dot{v}_{y1(d)} = -\frac{1}{m_d} \frac{dV_{d,\bar{d}}(r_{1,2})}{dy_1}, \quad \dot{v}_{z1(d)} = -\frac{1}{m_d} \frac{dV_{d,\bar{d}}(r_{1,2})}{dz_1} \quad (1c)$$

$$\dot{v}_{x2(\bar{d})} = -\frac{1}{m_{\bar{d}}} \frac{dV_{d,\bar{d}}(r_{1,2})}{dx_2}, \quad \dot{v}_{y2(\bar{d})} = -\frac{1}{m_{\bar{d}}} \frac{dV_{d,\bar{d}}(r_{1,2})}{dy_2}, \quad \dot{v}_{z2(\bar{d})} = -\frac{1}{m_{\bar{d}}} \frac{dV_{d,\bar{d}}(r_{1,2})}{dz_2} \quad (1c)$$

We assume that antiquarks follow equation of motion like the particles (e.g. do not move backwards in time as in Feynman diagrams), however, we apply the following quark exchange operations for quarks and antiquarks at a meson core, which may be analogues to the antimatter particles backwards motion. We assume that the quark and antiquark exchange positions and flip the sign of their velocities at the meson core defined by $V_{d,\bar{d}}(r_{1,2}) = 0$. We assume that inside the meson core a quark-gluon plasma is created by the coulomb potential singularity at $r_{1,2} = 0$ that we cannot model, and the quark exchange operation we define allow bypassing the singularity.

$$-\frac{1}{9} \frac{e^2}{4\pi \epsilon_0 d_{meson\ core}} + \sigma d_{meson\ core} = 0 \quad (2a)$$

$$d_{meson\ core} = \sqrt{\frac{e^2}{9(4\pi\epsilon_0)\sigma}} = \sqrt{\frac{\hbar c \alpha}{9\sigma}} \quad (2b)$$

$$r_d(t+1) = r_{\bar{d}}(t), \quad r_{\bar{d}}(t+1) = r_d(t) \quad (2c)$$

$$v_d(t+1) = -v_{\bar{d}}(t), \quad v_{\bar{d}}(t+1) = -v_d(t) \quad (2d)$$

We use the Bohr-Sommerfeld semiclassical quantization action integral to determine the initial conditions of the simulated quarks in the quark molecular dynamics scheme.

$$\left(n + \frac{1}{2}\right) \hbar = \sum_{q,\bar{q}} \oint_0^T \vec{p}_i \cdot d\vec{v}_i \quad (3)$$

Figure 1a-e below show the bound periodic meson classical trajectories for $d\bar{d}$, $u\bar{u}$ and the charged pion $\pi^- (d\bar{u})$. The meson symmetric initial conditions guarantee 0 total angular momentum and a trajectory of the quark and antiquarks towards a collision at short distance at half of the period. When the quarks reach the meson core, the quark exchange occurs according to equations 2c-d. The meson trajectory continues periodically and coherently where the quark and the antiquark switch paths and follow the path of each other.

$$E_{n=0}(\text{semiclassical})= 0.154 \text{ [GeV]}, X_0= 0.070 \text{ [fm]}, v_{y0}= 0.070 \text{ [} w * \text{ fm]}$$

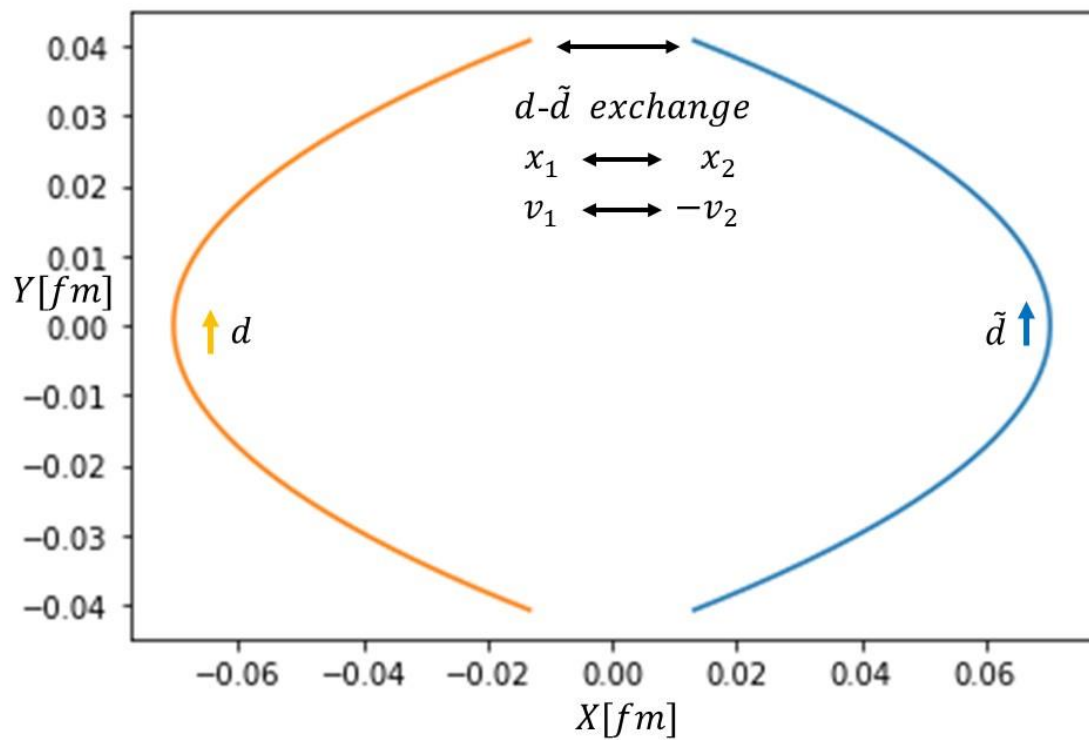


Figure 1a illustrates the first half of the meson periodic trajectory with quark exchanges in the upper part.

$$E_{n=0}(\text{semiclassical})= 0.154 \text{ [GeV]}, X_0= 0.070 \text{ [fm]}, v_{y0}= 0.070 \text{ [} w * \text{ fm]}$$

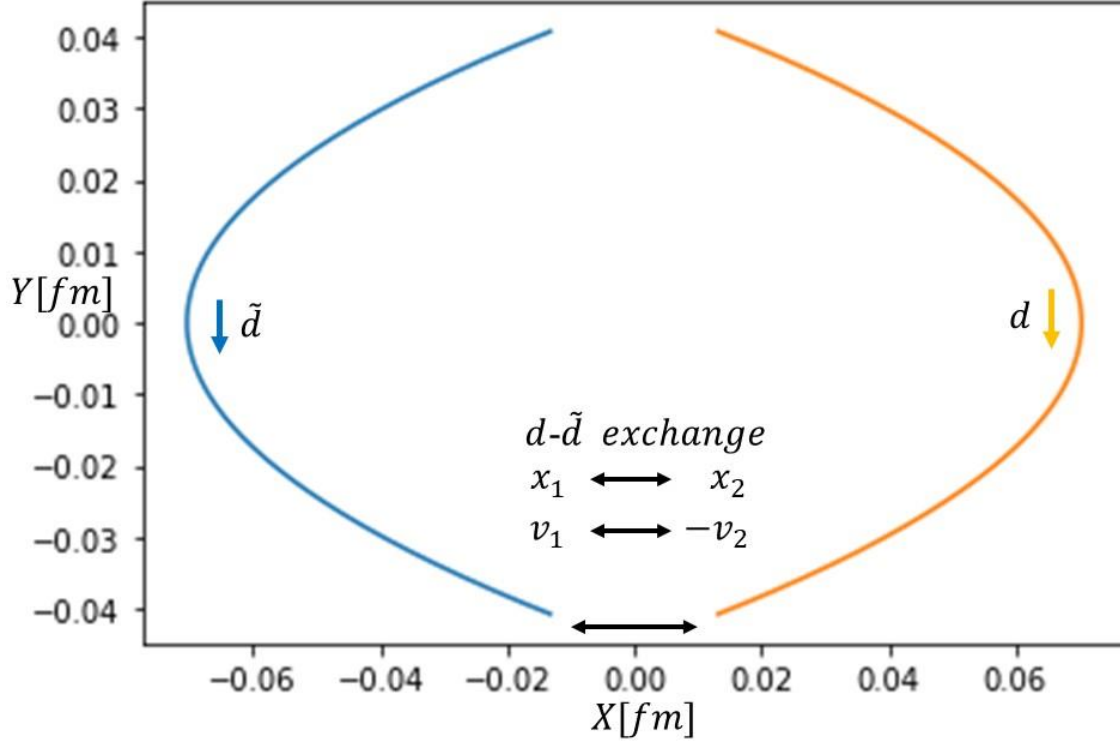


Figure 1b illustrates the second half of the meson periodic trajectory with quark exchanges in the lower part.

Using the Bohr-Sommerfeld semiclassical quantization action integral for the $d\tilde{d}$ meson and using the string tension $\sigma=1$ GeV/femtometer gives the meson energy/mass of 0.154 [GeV] where the exact value for the π^0 meson is 0.1349 GeV. The time period is $2.62e-24$ seconds which is on the same scale of Dirac's zitterbewegung time period of $6.72e-24$ seconds.

A second possible trajectory is a one-dimensional motion of the quark and antiquark along the X axis with 0 initial angular velocities. We calibrated the string tension parameter $\sigma = 0.74$ GeV/femtometer such that the energy of the π^- match the expected result in the literature of 0.1395 [GeV]. The time period was $3.523 \cdot 10^{-24}$. For the negatively charged π^- the core diameter

where the exchange operation occurs is $\sqrt{\frac{2e^2}{9(4\pi\epsilon_0)\sigma}}$.

$E_{n=0}(\text{semiclassical}) = 0.1395 \text{ [GeV]}, X_0 = 0.093 \text{ [fm]}$

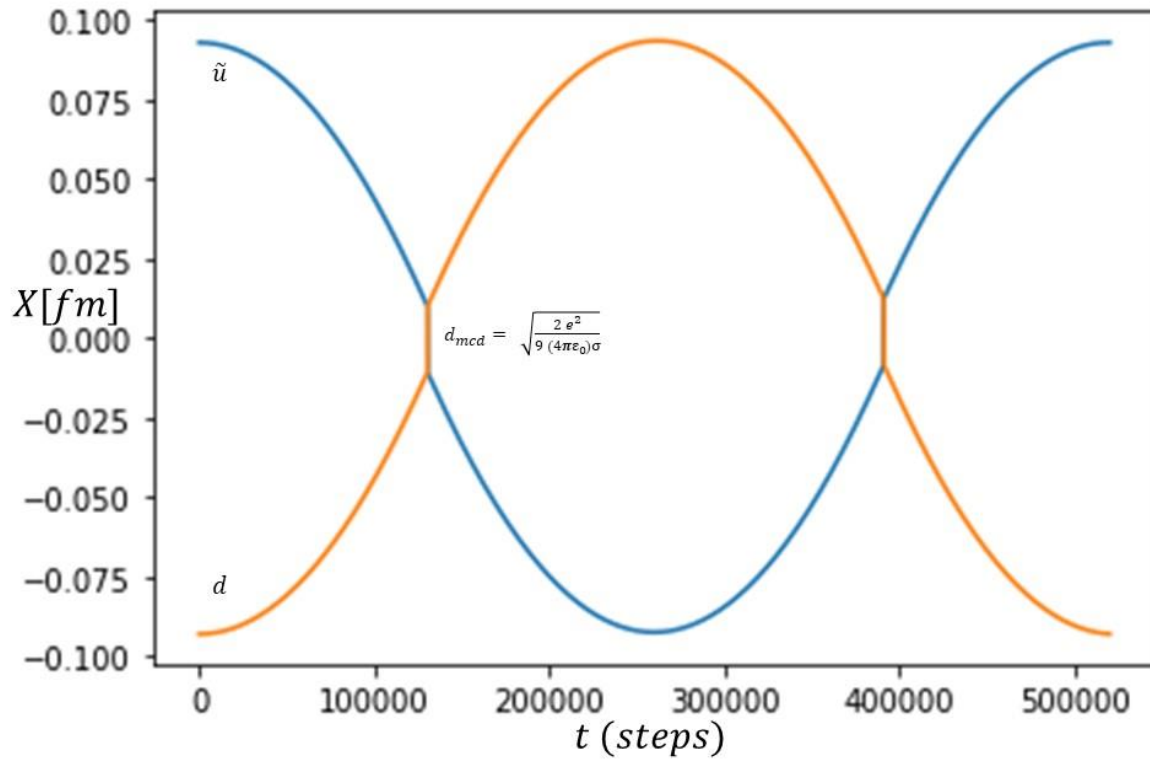


Figure 1c illustrates the charged meson π^- trajectory with calibrated string tension parameter of $\sigma = 0.74$ GeV/femtometer.

With the calibrated string tension parameter, we calculated the energies of the $d\tilde{d}$ and $u\tilde{u}$ mesons and got the same energy for both of 0.1340 [GeV] as shown below.

$$E_{n=0}(\text{semiclassical}) = 0.1340 \text{ [GeV]}, X_0 = 0.0911 \text{ [fm]}$$

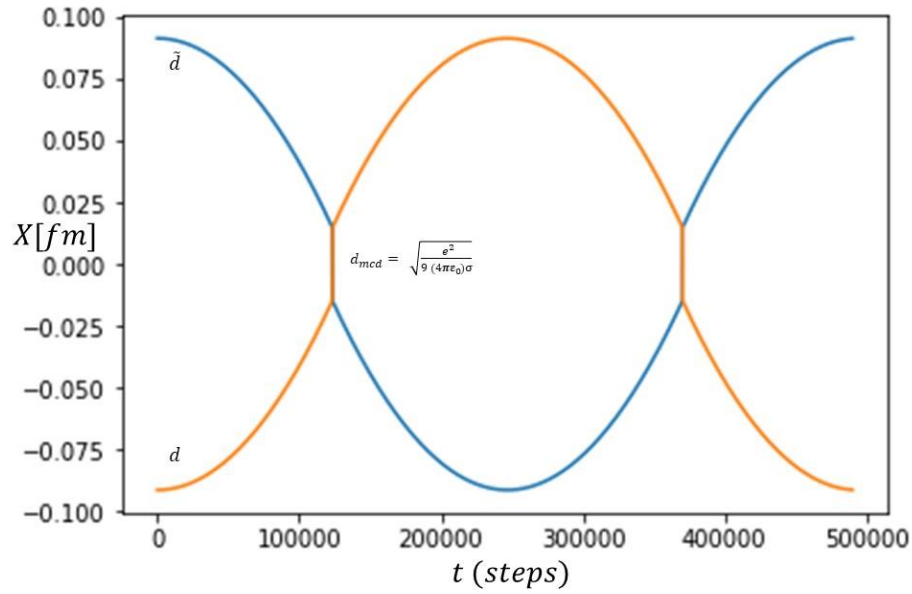


Figure 1d illustrates the $d\bar{d}$ meson symmetric trajectory moving inwards and outwards on the X axis with the quark exchanges at the meson core.

$$E_{n=0}(\text{semiclassical}) = 0.1340 \text{ [GeV]}, X_0 = 0.0911 \text{ [fm]}$$

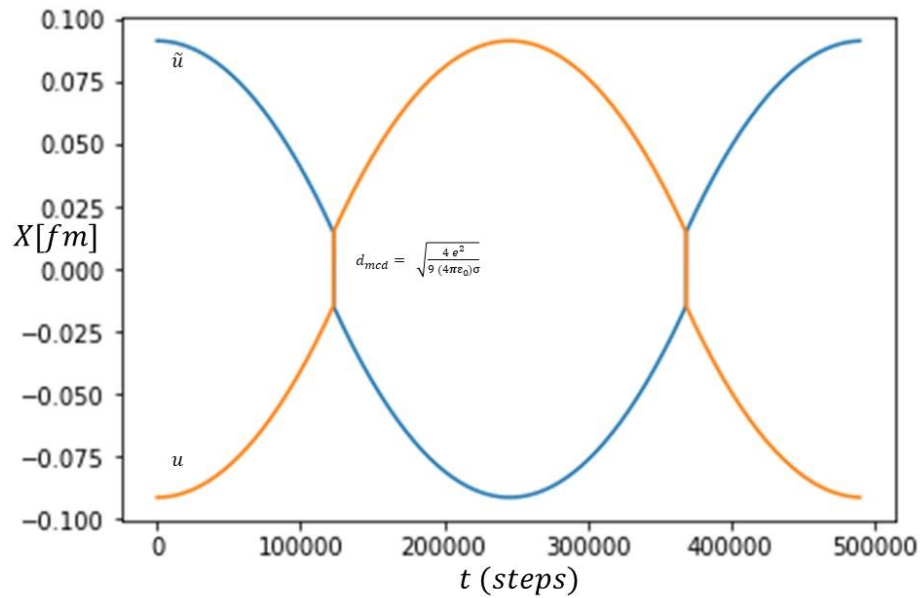


Figure 1e illustrates the $u\bar{u}$ meson symmetric trajectory moving inwards and outwards on the X axis with the quark exchanges at the meson core.

B. The Bound Pion Tetraquark Molecular Dynamics

The pion tetraquark molecule is assumed to be composed of a $d\bar{d}$ and $u\bar{u}$ mesons having a tetrahedron structure shown in figure 2. Two pion tetraquark tetrahedron enantiomers may exist obtained by exchanging the positions of two quarks at the vertices in line with the chiral symmetry of Weyl spinors and the effective chiral QCD theory vacuum¹⁵⁻²¹.

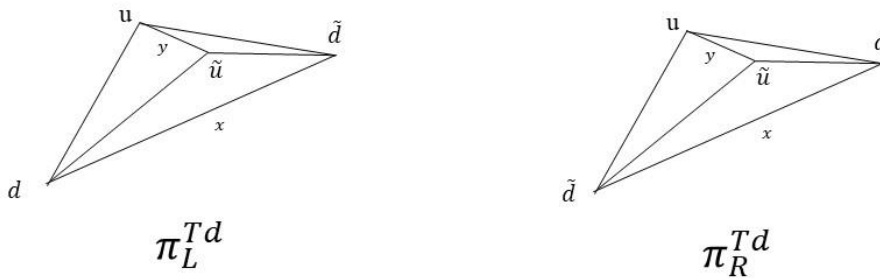


Figure 2 illustrates the two exotic pion tetraquark tetrahedron molecule enantiomers.

The pion tetraquark Hamiltonian includes kinetic energies, coulomb and the strong force string tensions terms between the quark pairs –

$$\begin{aligned}
H_{tetraquark} = & \frac{1}{2} m_u v_u^2 + \frac{1}{2} m_{\tilde{u}} v_{\tilde{u}}^2 + \frac{1}{2} m_d v_d^2 + \frac{1}{2} m_{\tilde{d}} v_{\tilde{d}}^2 - \frac{4}{9} \frac{e^2}{4\pi \epsilon_0 r_{u,\tilde{u}}} + \sigma r_{\tilde{u},u} + \\
& \frac{2}{9} \frac{e^2}{4\pi \epsilon_0 r_{u,\tilde{d}}} + \sigma r(u, \tilde{d}) - \frac{2}{9} \frac{e^2}{4\pi \epsilon_0 r_{u,d}} + \sigma r_{u,d} + \frac{2}{9} \frac{e^2}{4\pi \epsilon_0 r_{\tilde{u},d}} + \sigma r_{\tilde{u},d} - \frac{2}{9} \frac{e^2}{4\pi \epsilon_0 r_{\tilde{u},\tilde{d}}} + \sigma r_{\tilde{u},\tilde{d}} - \\
& \frac{2}{9} \frac{e^2}{4\pi \epsilon_0 r_{d,\tilde{d}}} + \sigma r_{d,\tilde{d}}
\end{aligned} \tag{4}$$

The exchange operation of quarks and antiquarks described above in equations 2a-d are applied for the meson at the pion core defined for each meson pair as follows.

$$d_{\tilde{d} \text{ meson}} = \sqrt{1/9 \frac{\hbar c \alpha}{\sigma}} = 0.0126 \text{ fm} \tag{5a}$$

$$d_{\tilde{u}u \text{ meson}} = \sqrt{4/9 \frac{\hbar c \alpha}{\sigma}} = 0.0253 \text{ fm} \tag{5b}$$

The exotic pion tetraquark periodic trajectory is shown in figure 3. The two-meson quark and antiquark, $u\tilde{u}$ and $\tilde{d}d$, follows a meson like trajectory rotated by 90 degrees along the X and Y axes. The quarks exchange positions and flip their velocities at the pion tetrahedron core and the quarks and antiquarks continue with the periodic trajectory. By selecting the initial positions of the pion tetraquark and carefully matching the exchange operation timings that occur at the pion tetraquark core, a bound state energy of the pion tetraquark of 0.2194 [GeV] is obtained with a binding energy of about 0.0486 [GeV] comparing to the free di-meson $d\tilde{d}$ and $u\tilde{u}$ energies of 0.134 [GeV] each. We note that the Bohr-Sommerfeld action integral (Eq. 3) cycle time is doubled to get the ground state value of $\frac{1}{2} \hbar$ and the period is 1.587e-24 seconds.

$$E_{n=0}(\text{semiclassical}) = 0.220 \text{ [GeV]}, u_0(y) = 0.0295 \text{ [fm]}, d_0(x) = 0.018 \text{ [fm]}$$

$$E_b(\text{pion tetrahedron}) = 0.2194 - (0.134 + 0.134) = -0.0486 \text{ [GeV]}$$

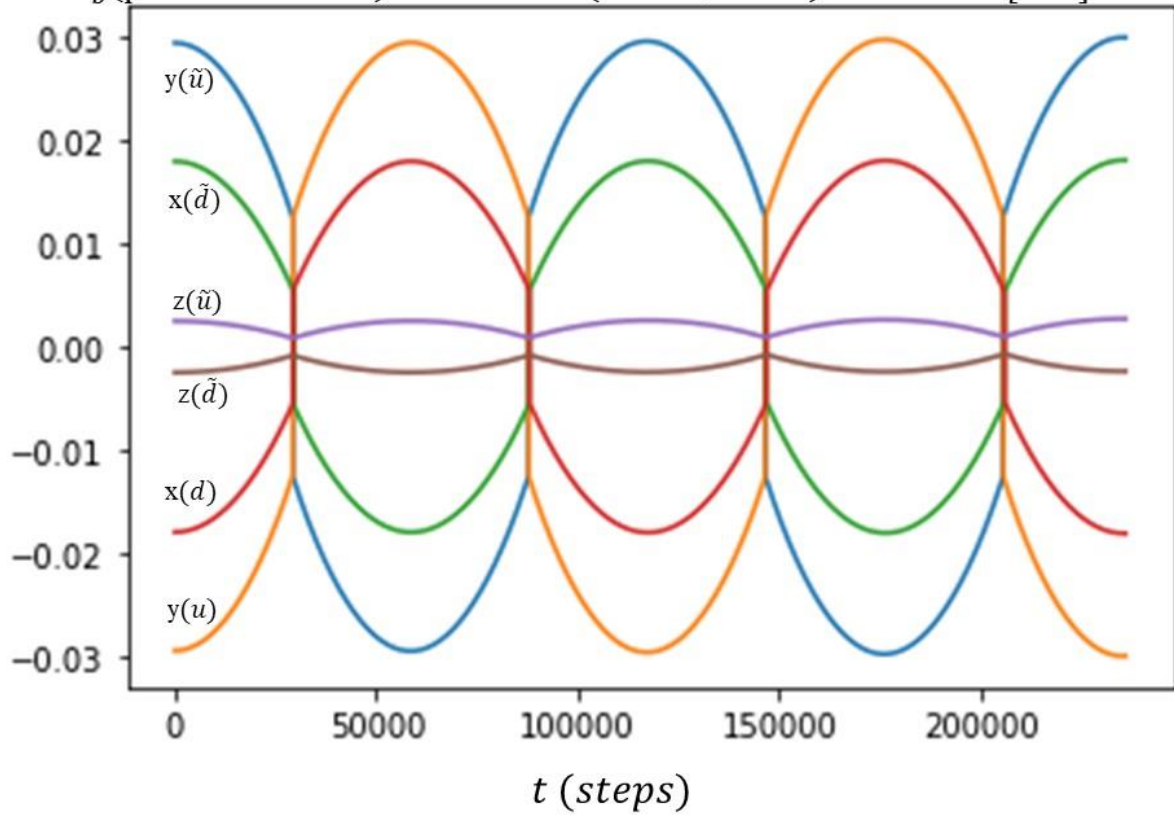


Figure 3a illustrates the exotic pion tetraquark tetrahedron coherent trajectory where the quark exchanges at the pion core surface occur simultaneously and the motion of the Z axis.

Figure 3b shows the stability of the exotic pion tetrahedron periodic solution for 10 cycles.

$$E_{n=0}(\text{semiclassical}) = 0.220 \text{ [GeV]}, \quad u_0(y) = 0.0295 \text{ [fm]}, \quad d_0(x) = 0.018 \text{ [fm]}$$

$$E_b(\text{pion tetrahedron}) = 0.2194 - (0.134 + 0.134) = -0.0486 \text{ [GeV]}$$

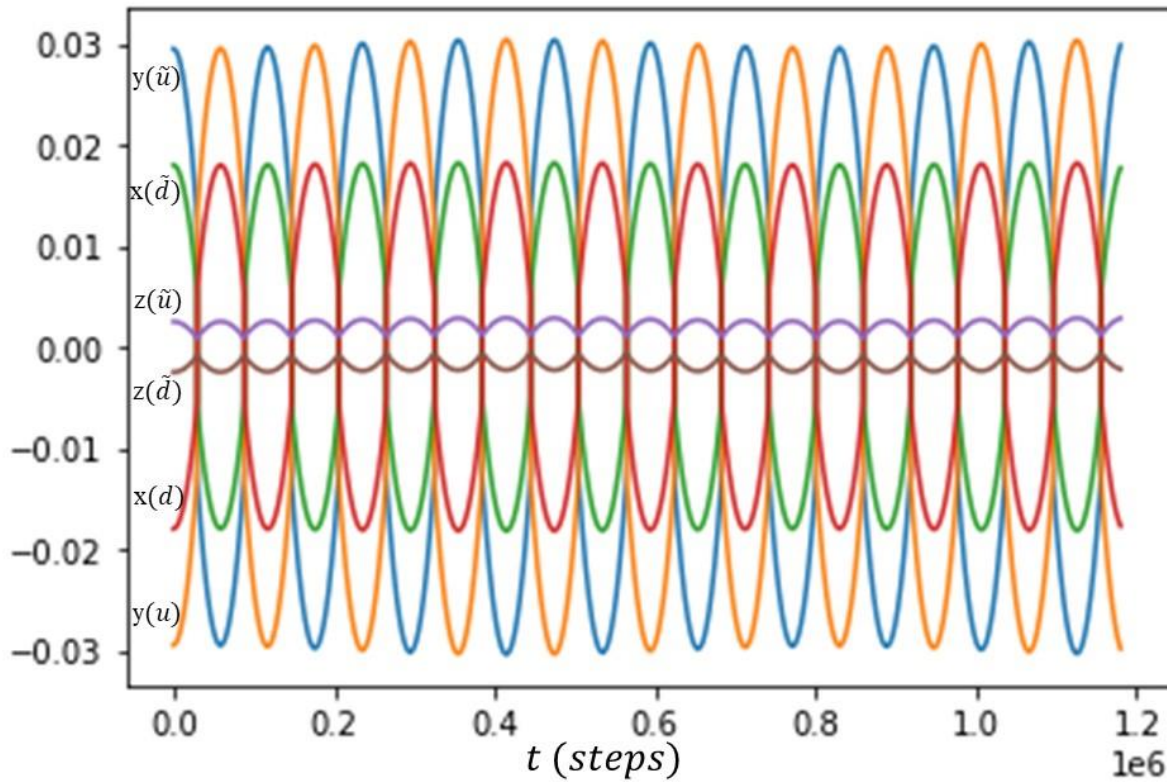


Figure 3b illustrates the exotic pion tetraquark tetrahedron periodic solution stability.

Note that we can use the pion tetrahedron potential energy of equation 6 to determine the pion tetrahedron core diameters as a function of the initial elevation between the two mesons in the tetrahedron configuration.

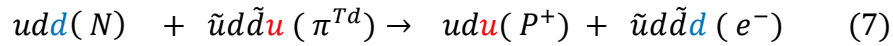
$$\begin{aligned}
V_{u,\tilde{u},d,\tilde{d}}(r_{u,\tilde{u}}, r_{d,\tilde{d}}, Z) &= 0 \\
&= -\frac{4}{9} \frac{e^2}{4\pi \varepsilon_0 r_{u,\tilde{u}}} + \sigma r_{\tilde{u},u} + \frac{2}{9} \frac{e^2}{4\pi \varepsilon_0 r_{u,\tilde{d}}} + \sigma r(u, \tilde{d}) - \frac{2}{9} \frac{e^2}{4\pi \varepsilon_0 r_{u,d}} + \sigma r_{u,d} \\
&+ \frac{2}{9} \frac{e^2}{4\pi \varepsilon_0 r_{\tilde{u},d}} + \sigma r_{\tilde{u},d} - \frac{2}{9} \frac{e^2}{4\pi \varepsilon_0 r_{\tilde{u},\tilde{d}}} + \sigma r_{\tilde{u},\tilde{d}} - \frac{2}{9} \frac{e^2}{4\pi \varepsilon_0 r_{d,\tilde{d}}} \\
&+ \sigma r_{d,\tilde{d}} \tag{6}
\end{aligned}$$

For each Z value that may depend on external fields such as the electromagnetic or gravitational fields, the pion tetrahedron potential energy may be set to 0 by selecting the two other distances $r_{u,\tilde{u}}$, $r_{d,\tilde{d}}$ appropriately. Hence infinite number of pion tetrahedron particles in the vacuum will have 0 energy. We assume that in the vicinity of a massive body, the pion tetraquark tetrahedron fabric may have higher density and spherical symmetry according to the applied gravitational or electrical field. Near a black hole for example, the pion tetraquark tetrahedron fabric may be extremely dense, where far away from any galaxy in cosmic voids²²⁻²⁴, the pion tetraquark tetrahedron vacuum fabric may be extremely diluted.

Note that since the mesons switch positions along the X or Y axes, the two pion tetrahedron enantiomers shown in figure 2 are dynamically mixed, the tetrahedron chiral symmetry is broken as expected with the spontaneous breaking of the chiral symmetry of the QCD vacuum.

4. The Electron and the Pion Tetraquark Tetrahedron Cloud

Assuming that the β decay is a second order scattering reaction triggered by the vacuum pion tetraquark tetrahedrons, the β decay generates a proton and a negatively charged exotic tetraquark, $\tilde{u}d\tilde{d}d$.



The reaction equation conserves quark number and flavor, and the exotic negatively charged tetraquark, $\tilde{u}d\tilde{d}d$, may be a non-elementary, non-point like electron. A first electron tetraquark state may be $\tilde{u}dd\tilde{d}$, and a second electron tetraquark state may be $\tilde{u}du\tilde{u}$ ⁹⁻¹³. Transforming an electron to a pion tetraquark tetrahedron on the vacuum fabric may occur by quark flavor exchanges between two adjacent fabric sites. A pion tetraquark tetrahedron may be transformed by quark flavor exchange to an electron tetraquark tetrahedron and vice versa by quark exchange reactions. Since the quark exchange reactions are symmetric, e.g. the reactants and products are identical as shown in equation 9 below, a double well potential model²⁵ may be used to represent the reaction like in the ammonia molecule inversion²⁶. Accordingly, the motion of the electron tetraquark tetrahedron on the pion tetraquark tetrahedron fabric may occur via tunneling through potential barrier. The u and d quarks are exchanged as illustrated in figure 5 below.

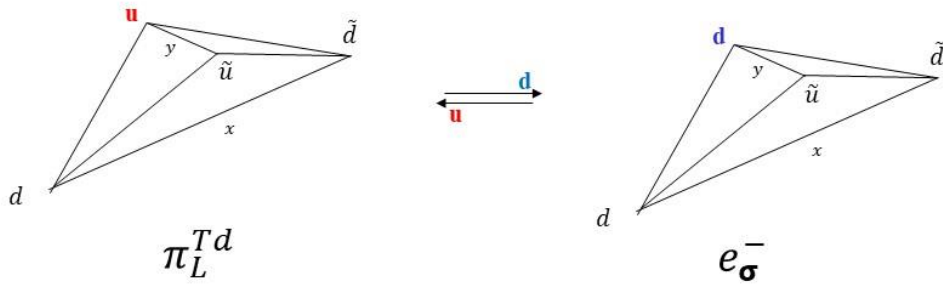


Figure 5 illustrates an electron tetraquark and a pion tetraquark tetrahedron exchanging quark flavors (**u** and **d**).

A. The Electron Tetraquark Molecular Dynamics

The electron tetraquark tetrahedron system is simulated first with quark molecular dynamics. The $\tilde{d}d$ meson trajectory is along the X axis and the charged $\tilde{u}d$ pion, π^- , trajectory is along the Y axis. The electron tetraquark tetrahedron trajectory is shown in figures 6. For the electron tetraquark, the $\tilde{d}d$ and $\tilde{u}d$ quark exchanges occurs at the different diameters given below.

$$d_{\tilde{d}d \text{ meson}} = \sqrt{1/9 \frac{\hbar c \alpha}{\sigma}} = 0.0126 \text{ fm}, \quad d_{\tilde{u}d \text{ meson}} = \sqrt{2/9 \frac{\hbar c \alpha}{\sigma}} = 0.0178 \text{ fm} \quad (8)$$

A bound state energy of the electron tetraquark of 0.250 [GeV] is obtained, lower by about 0.023 [GeV] from the free $d\tilde{d}$ and $d\tilde{u}$ mesons of 0.134 [GeV] and 0.1395 [GeV]. The Bohr-Sommerfeld action integral is only 0.07 \hbar which is too low for the electron tetraquark ground state.

However, we assumed above that the electron and pion tetraquarks perform rapid u and d quark exchanges and hence the Bohr-Sommerfeld action integral should be taken over many pion tetraquarks sites that will produce the expected value of $\frac{1}{2}\hbar$.

$$E_{n=0}(\text{semiclassical}) = 0.250 \text{ [GeV]}, \quad u_0(y) = 0.01105 \text{ [fm]}, \quad d_0(x) = 0.01019 \text{ [fm]}$$

$$E_b(\text{electron tetrahedron}) = 0.250 - (0.134 + 0.139) = 0.023 \text{ [GeV]}$$

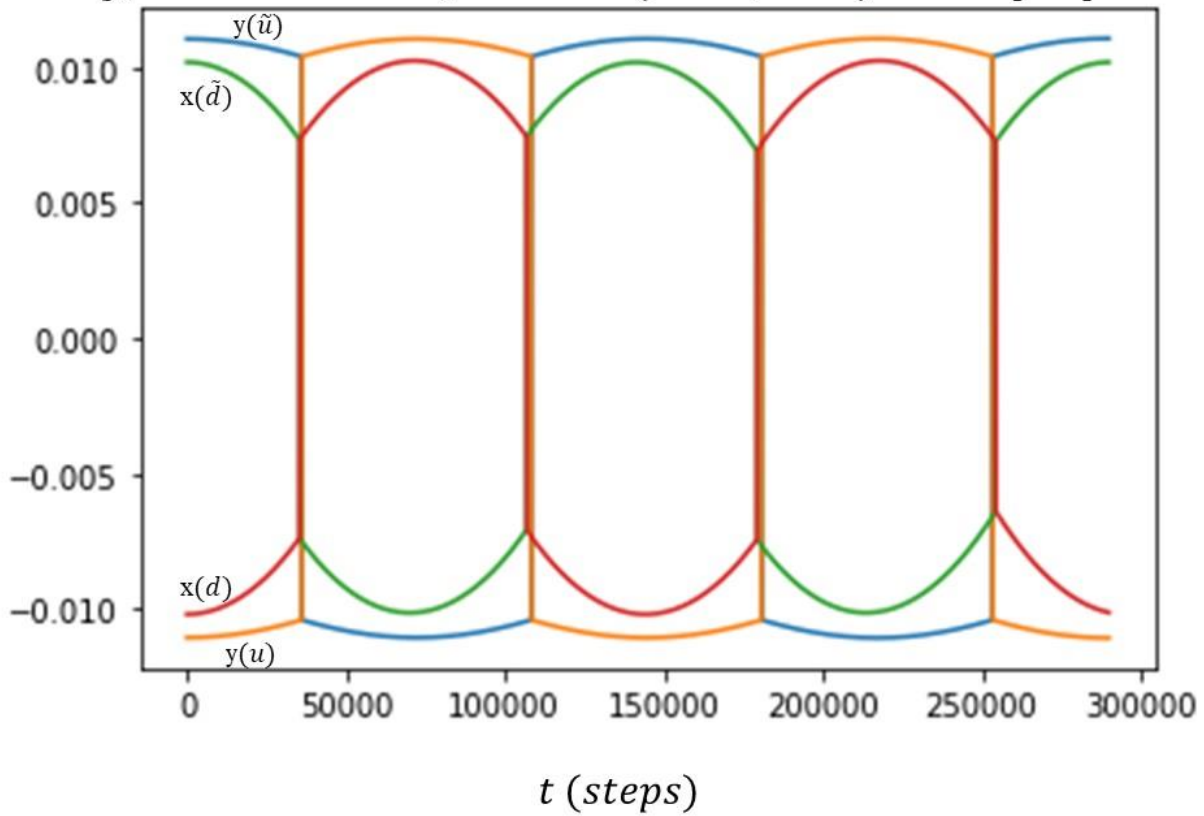


Figure 6 illustrates the electron tetraquark tetrahedron coherent trajectory for small number of periods.

B. The Electron and Pion Tetraquark Tetrahedron Double Well Potential Model

The pion and electron exotic tetraquarks scattering reaction between two fabric sites i and j are described in equation 9 where the d and the u quarks are exchanged. Since the reactants and products are identical a double well potential model may be used.

$$\tilde{u}d\tilde{d}d (e^L)_i + \tilde{u}d\tilde{d}u (\pi^{Td})_j \rightarrow \tilde{u}d\tilde{d}u (\pi^{Td})_i + \tilde{u}d\tilde{d}d (e^L)_j \quad (9)$$

In the case of the second electron exotic tetraquark state (R), the \tilde{u} and \tilde{d} antiquarks may be exchanged according to the following scattering reaction.

$$\tilde{u}d\tilde{d}u (\pi^{Td})_i + \tilde{u}d\tilde{u}u (e^R)_j \rightarrow \tilde{u}d\tilde{u}u (e^R)_i + \tilde{u}d\tilde{d}u (\pi^{Td})_j \quad (10)$$

A quantum mechanical solution for the electron and pion tetraquark tetrahedron double well potential model²⁵ is presented below and extended further to a cloud of pion tetraquarks.

$$\hat{H} = \frac{\hat{p}^2}{2m_e} + m_e \lambda (\hat{x}^2 - a^2)^2 \quad (11)$$

m_e is the electron rest mass, $2a$ is the distance between pion tetrahedron sites and the coupling parameter λ may be determined by the potential barrier height, $V_0 = m_e \lambda a^4$, where $V_0 = \hbar\omega_z = 2m_e c^2$. The frequency $\omega_z = \frac{2m_e c^2}{\hbar}$ is Dirac's free space trembling motion frequency, the zitterbewegung²⁷⁻²⁸.

Figure 7 below illustrates the double well potential for the electron tetraquark tetrahedron and the pion tetraquark tetrahedron quark flavor exchange reaction in adjacent fabric sites i and j . With the quantum mechanical double well potential model, the electron motion in the vacuum fabric is via tunneling through the potential barrier V_0 . The barrier height $V_0 = 2m_e c^2$ is twice the electron rest mass energy, which is the threshold for electron-positron pair production. Note that the electron tetraquarks on both sides of the double well are identical and hence the electron state (

and $E_s = 0.7004 \hbar\omega$ is a bound state inside the potential well. The tunneling time is $5.849 * 10^{-21}$ seconds.

$$T_{tunneling} = \frac{\pi\hbar}{E_a - E_s} = 5.849 * 10^{-21} \text{ seconds} \quad (12)$$

A superposition of the symmetric and antisymmetric eigenstates is taken as the initial state $\psi_{t=0}$ describing an electron wavepacket located in the left well initially.

$$\psi_0 = \frac{1}{\sqrt{2}} (\psi_s + j \psi_a) \quad (13)$$

After a half period the electron wavepacket tunnels to the right well

$$\psi_{T_p/2} = \frac{1}{\sqrt{2}} (\psi_s e^{-iE_s T_p/2} + j \psi_a e^{-iE_a T_p/2}) \quad (14)$$

The electron wavepacket continues oscillating between the two wells with a period of $T_p = \frac{2\pi\hbar}{E_a - E_s}$.

The electron velocity in the fabric may be calculated by dividing the distance between two adjacent wells, $2a$, by the tunneling time.

$$v_e = \frac{2a}{T_{tunneling}} = \frac{2a (E_a - E_s)}{\pi\hbar} = 0.44 c \left[\frac{m}{sec} \right] \quad (15)$$

Note that the electron velocity here is about half of the speed of light and that the tunneling frequency is on the time scale of the free space trembling motion frequency, the zitterbewegung, similar to the electron semi-classical models²⁷⁻²⁸.

5. The Electron and Pion Tetraquark Tetrahedron Cloud

The single electron and pion tetraquark tetrahedron double well potential model may be extended to the vacuum fabric where the electron with the vacuum pion tetraquark tetrahedrons are assumed to form a dense and polarized sphere. In the center of the sphere, the double well potential model length may be extremely small below the Compton length. Away from the cloud center, the distance between pion tetraquark tetrahedron may increase and the pion tetraquark

tetrahedron density is reduced. After about few Compton lengths, the distance between pion tetraquark tetrahedron is such that the quark exchange reactions stop. The electron tunneling is exponentially decreased and the electron is trapped in the cloud by the lack of quark exchange reactions outside. The electron is confined by the vacuum pion tetraquark tetrahedron fabric/cloud.

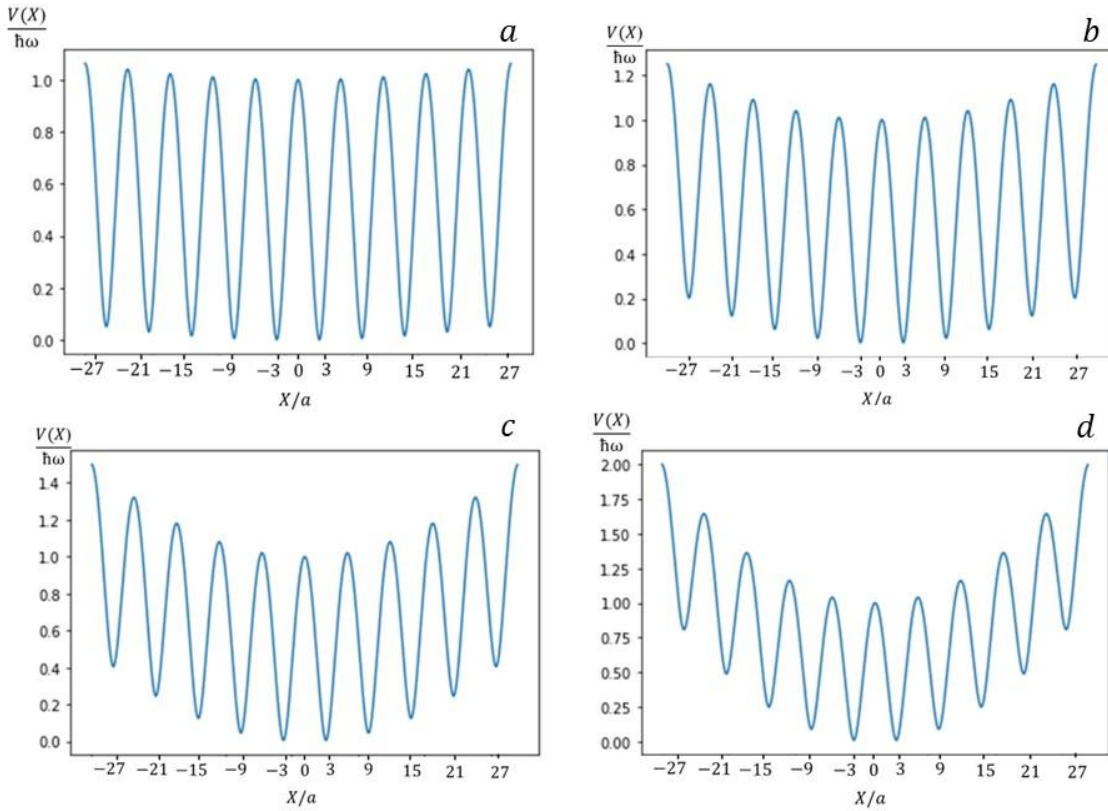
The following table summarizes results with increasing distance between the two potential wells, $2a$, $4a$ and $6a$ keeping the potential barrier height at the same value, $V_0 = 2m_e c^2$, by changing the value of the coupling parameter λ , $\lambda = \frac{2c^2}{a^4}$, $\lambda = \frac{2c^2}{16a^4}$ and $\lambda = \frac{2c^2}{81a^4}$.

Distance between the two wells	$E_a/\hbar\omega$	$E_s/\hbar\omega$	$T_{tunneling}(\text{sec})$
$2a$	1.0463	0.7004	5.849510^{-21}
$4a$	0.4741	0.4502	8.457710^{-20}
$6a$	0.318497	0.31698	1.34040^{-18}

The electron tunneling time between the two wells is reduced significantly with the growth of the distance between the wells. With the $6a$ distance the tunneling is about 229 times slower than with $2a$ distance (a is defined as the electron Compton length $\frac{\hbar}{m_e c}$). The extremely fast electron wavepacket dynamics in the vacuum fabric may be observed in the future with the new attosecond electron microscopy²⁸.

The electron charge polarizes the pion tetraquark tetrahedrons sphere since the pion tetraquark tetrahedrons have built in electric dipole moments. We assume that the polarization of the vacuum pion tetraquark tetrahedrons cloud by the electron adds a long-range harmonic potential term $\sim \frac{\hbar\omega x^2}{L^2}$, where L is the length scale of the pion tetraquarks cloud.

The electron and pion tetraquark tetrahedron potential is extended in one dimension with 10 fabric sites and with increasing long-range harmonic potential term, 0.25, 1, 2 and 4 $\frac{\hbar\omega x^2}{L^2}$ for the cloud model.



Figures 8a-d illustrates the electron and pion tetraquark tetrahedron cloud potential in one dimension with 10 fabric sites and increasing long- range harmonic potential term ((a) 0.25, (b) 1, (c) 2 and (d) 4 $\frac{\hbar\omega x^2}{L^2}$).

The two lowest symmetric, ψ_1 , and antisymmetric, ψ_2 , eigenfunctions are shown below for the four long-range harmonic potential values. Note that the eigenfunctions peaks are localized in the fabric wells and that in the two lower states, the tetraquark electron is not localized in a single well, it has a finite probability to be found in few adjacent wells in the fabric.

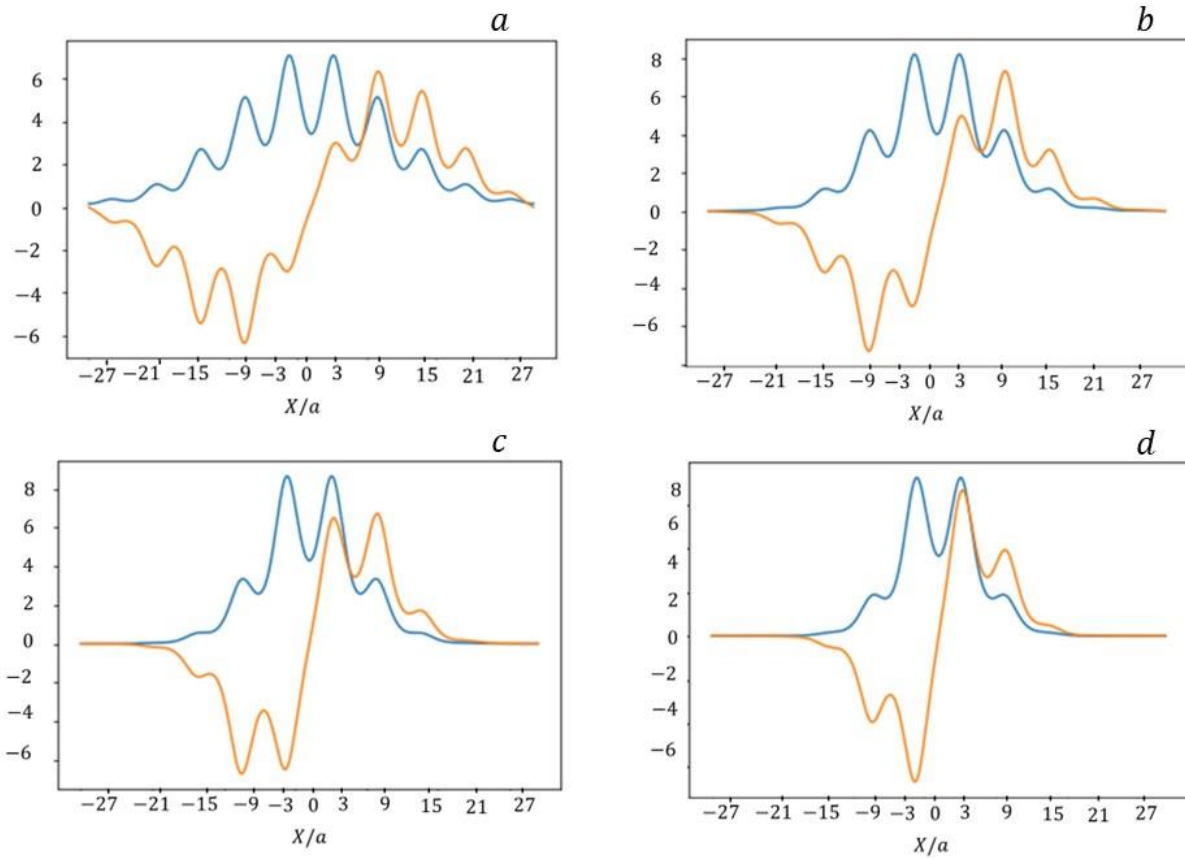


Figure 9a-d illustrates the first and second symmetric ψ_1 and antisymmetric ψ_2 eigenfunctions for the four long range harmonic potential values ((a) 0.25, (b) 1, (c) 2 and (d) $4 \frac{\hbar\omega x^2}{L^2}$).

An initial wavepacket may be formed by a superposition of the two lower symmetric and antisymmetric eigenstates, $\psi_0 = \frac{1}{\sqrt{2}}(\psi_1 + j\psi_2)$. The electron wavepacket has high probability to be found in the first few wells on the left initially. After half a period, the wavepacket tunnels to the right-hand side wells (in blue). Note that with higher value of the long-range harmonic potential the low eigenstates are localized mainly in a single fabric site as shown in figures 10d.

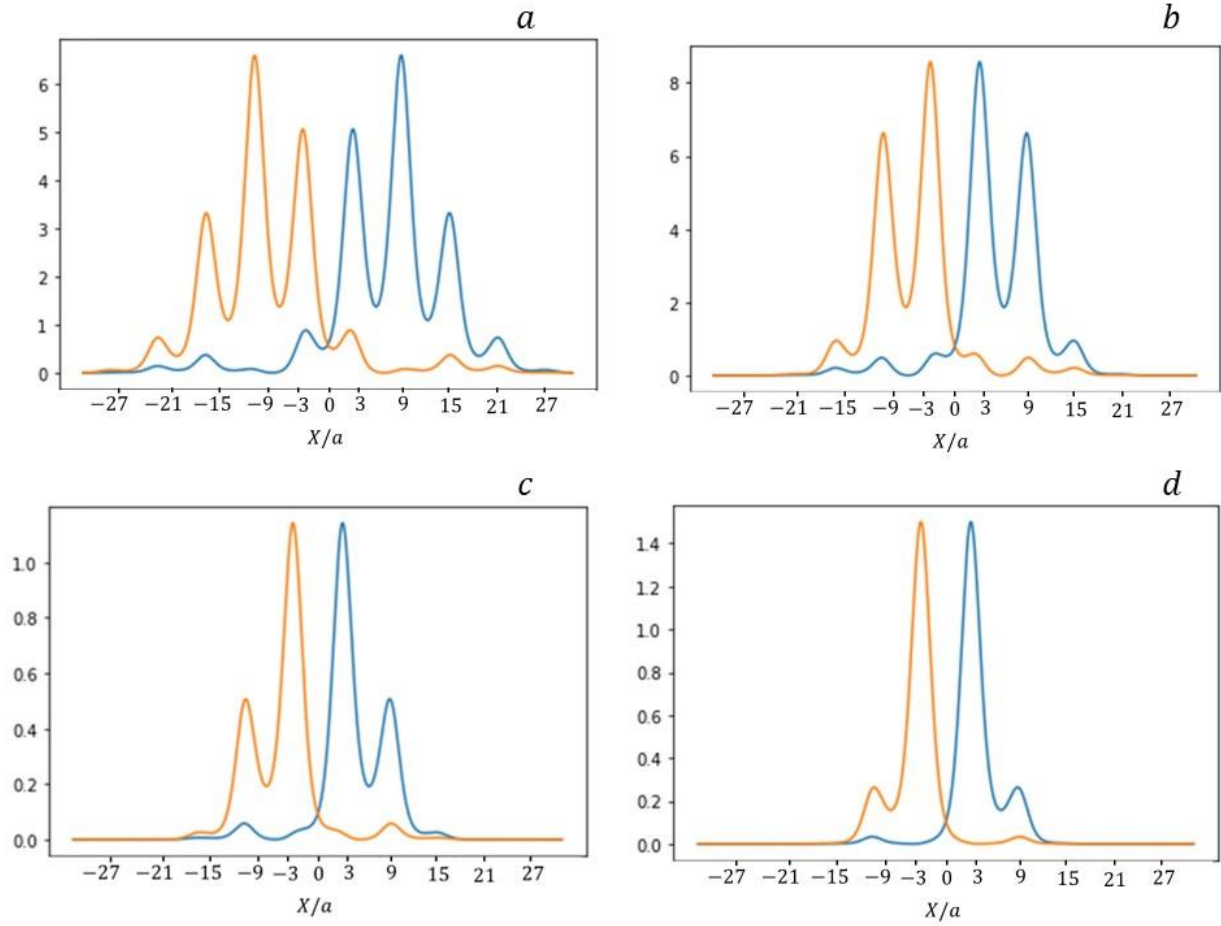


Figure 10a-d illustrates the electron wavepacket at $t=0$ (in orange) and after a half time period (in blue) for the four long-range harmonic potential values ((a) 0.25, (b) 1, (c) 2 and (d) $4 \frac{\hbar\omega x^2}{L^2}$).

The position expectation value of the electron wavepacket for 5 time periods for the four long-range harmonic potential values calculated according to equation 16 are shown in figures 11a-d.

$$X(t) = \langle \psi_t | \hat{X} | \psi_t \rangle \quad (16)$$

The position expectation value oscillates between the left-hand side wells to the right-hand side wells. With higher long-range harmonic potential values the oscillation amplitude decreases since the wavepackets are more localized in the first wells.

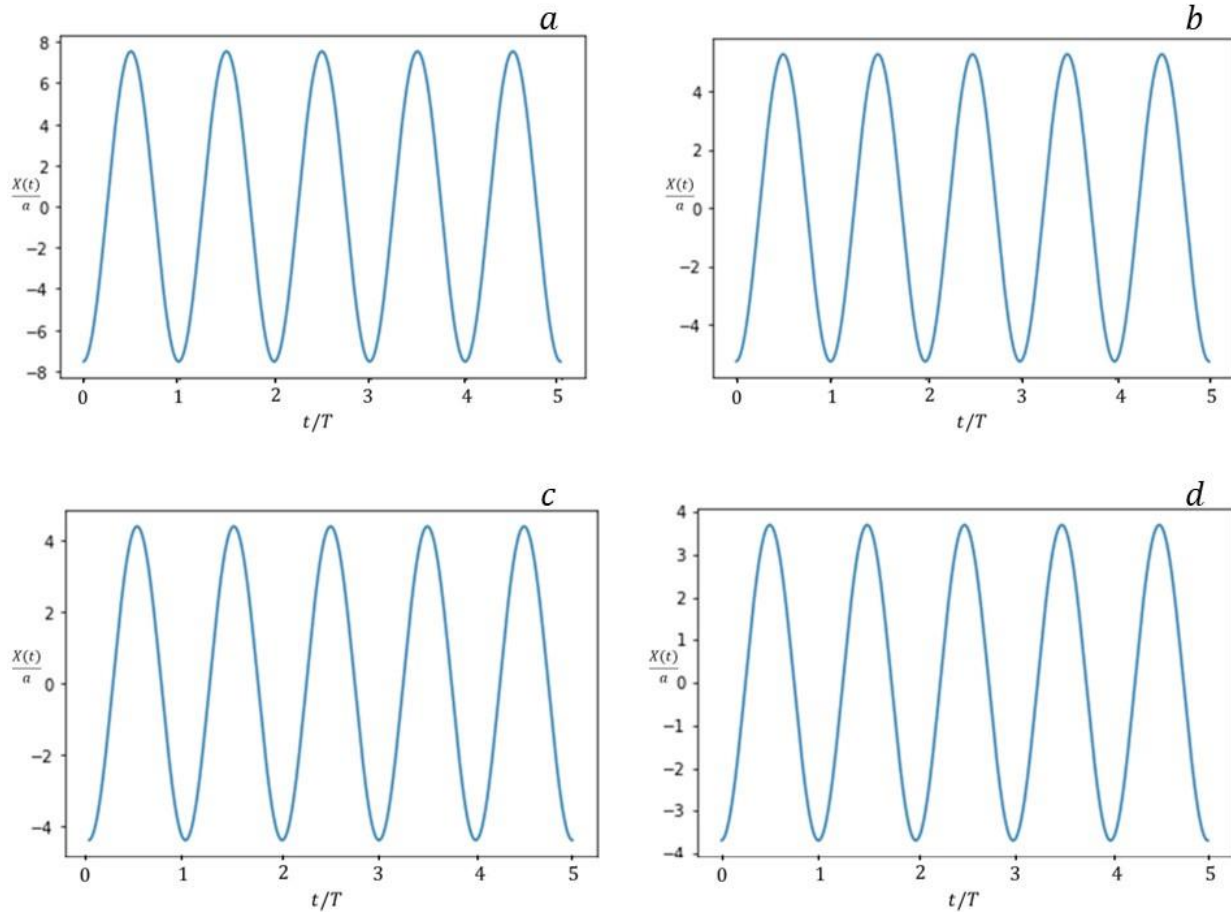


Figure 11a-d illustrates the position expectation value of the electron wavepacket for 5 time periods for the four long -range harmonic potential values ((a) 0.25, (b) 1, (c) 2 and (d) $4 \frac{\hbar\omega x^2}{L^2}$).

The higher symmetric ψ_7 and antisymmetric ψ_8 eigenstates are localized in the outer wells. The superposition, $\psi_0 = \frac{1}{\sqrt{2}} (\psi_7 + j\psi_8)$, is shown below where the tunneling occurs now between the outer wells.

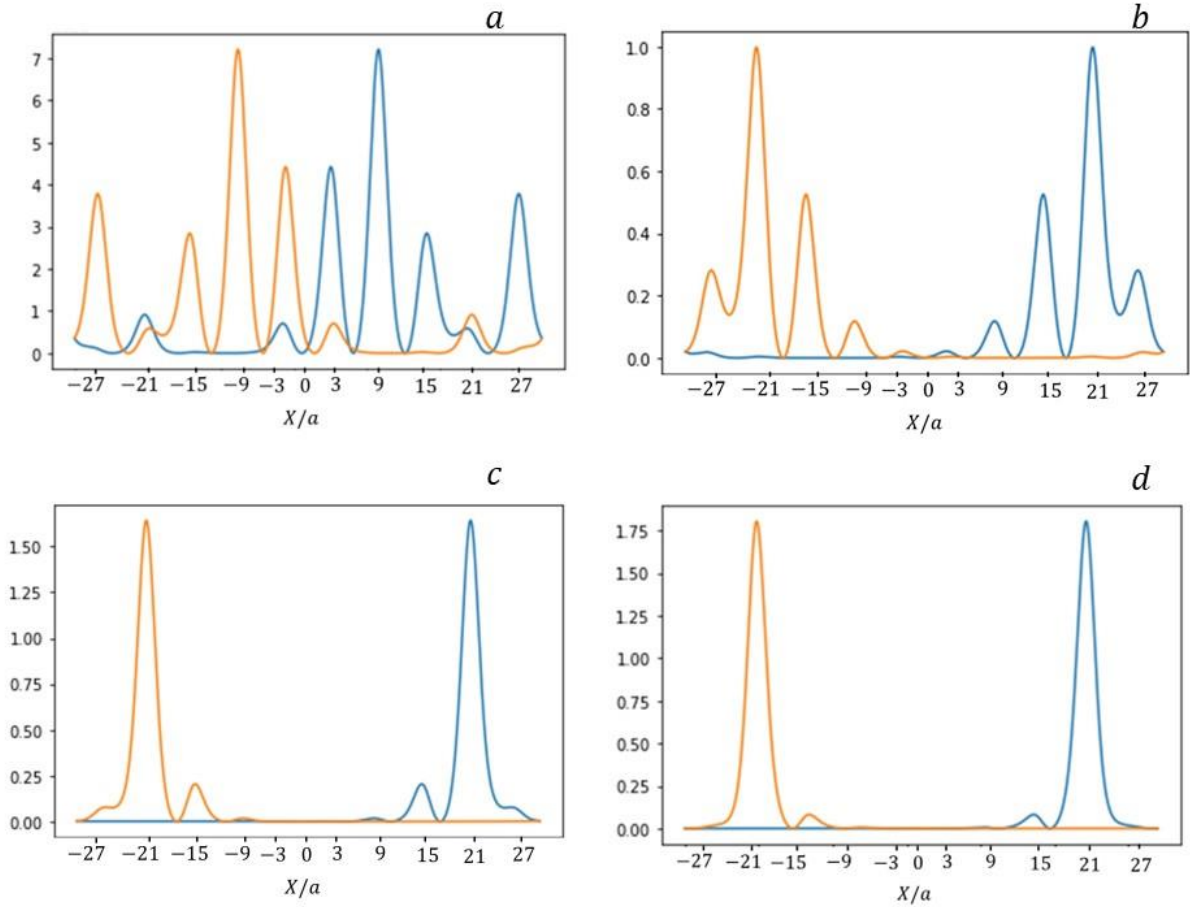


Figure 12a-d illustrates the electron wavepacket at $t=0$ (in orange) and after half time period (in blue) for the four long -range harmonic potential values ((a) 0.25, (b) 1, (c) 2 and (d) $4 \frac{\hbar\omega x^2}{L^2}$).

We assume that the polarization effect of the charged electron on the vacuum fabric is to rearrange the pion tetraquark tetrahedron sphere with the speed of light around the electron site. The length parameter a may be changed numerically ($\sim 0.46 \frac{\hbar}{m_e c}$ for example) such that the calculated electron velocity according to equation 11, $v_e = \frac{2a(E_a - E_s)}{\pi\hbar}$, will be close to the speed of light. In this case, the rearrangement of the pion tetrahedrons cloud and the tunneling of the electron wavepacket occurs at maximal $\frac{\hbar\omega x^2}{L^2}$ speed and the electron speed is limited to c since the pion tetrahedrons fabric cannot rearrange faster.

The electron tunnels from site to site extremely fast with the zitterbewegung frequency and it cannot be isolated. Schrödinger suggested that the electron particles would be described with wavepackets and found that a Gaussian wavepacket formed by a linear combination of plane waves gets wider linearly with time in free space¹. The electron wavepacket simulations above do not prove the proposed quark model for the electron and pion tetraquark tetrahedron vacuum fabric but show that a confined electron wavepacket may be obtained with the duplicated double well potential model that represents the electron and the vacuum pion tetraquark tetrahedron cloud. Lattice QCD may allow calculating the mass of the electron and pion tetraquarks and support the proposed quark model of the electron and the pion tetrahedron vacuum. With the proposed model, the electron is never bare like Dirac assumed and we suggest that the perturbative free particle bare propagator may be the cause for the divergence of the vacuum polarization and electron self-energy Feynman integrals that do not occur if the pion tetraquark fabric is added²⁹⁻³¹.

6. The Positron Tetraquark Tetrahedron

The positrons tetraquark tetrahedrons have a positive charge of a u and \tilde{d} quarks replacing the negative charge of a \tilde{u} and d quarks of the electron tetraquark tetrahedrons as shown below in figures 13 (a-b) for the electrons on the left and for the positrons on the right in figures 13 (c-d). Two positron enantiomers, e_R^+ and e_L^+ , may exist like the two electron tetraquark tetrahedron enantiomers e_R^- and e_L^- . In the four cases, quark exchanges transform the electrons, or the positrons, to a pion tetraquark tetrahedron (π^{Td}) and vice versa conserving charge and tetraquark state.

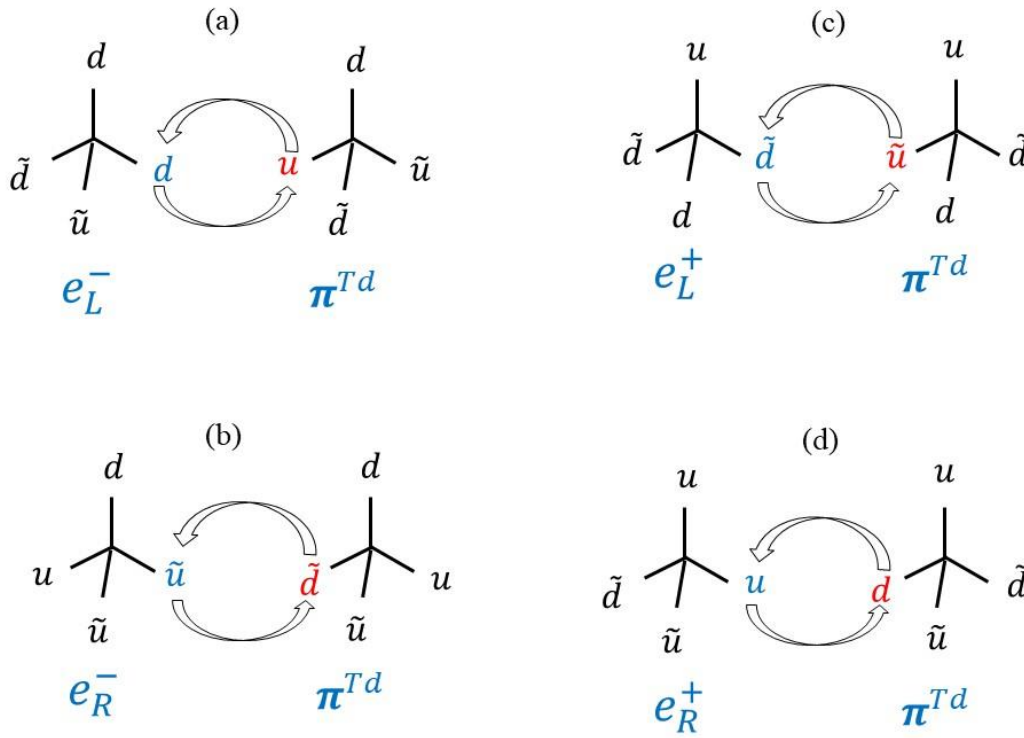
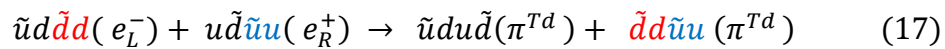


Figure 13 illustrates electron tetraquark tetrahedron enantiomers (a) and (b) and positron tetraquark tetrahedron enantiomers (c) and (d) exchanging quarks with pion tetraquark tetrahedrons with symmetric reactions such that the electrons and positrons transform to pion tetraquark tetrahedrons and vice versa conserving charge and chiral state.

7. Electron-Positron Decay

Electron-positron tetraquarks tetrahedrons decay on the pion tetraquark tetrahedron fabric may occur by scattering of an electron tetraquark tetrahedron and a positron tetraquark tetrahedron forming two neutral pion tetraquark tetrahedrons that become part of the vacuum pion tetrahedron fabric as shown in equation 17.



An electron tetrahedron in site i on the fabric collides with a positron tetraquark on adjacent site j and the outcome is that in both i and j sites after the collision will have pion tetraquark tetrahedrons, where the electron and positron charges and spins are annihilated. The extra energy

of the electron and positron may be transferred to the vacuum pion tetraquark tetrahedron fabric as electromagnetic wave energy for example. Note that in equation 17 the number and flavor of the quarks are conserved. The quarks are not destroyed nor created in these quark exchanges⁹⁻¹³.

8. Lattice QCD and the Quark Model of the Electron

Lattice QCD is a non-perturbative computation scheme for the strong force³⁴⁻³⁷. Perlovsek et al³⁵ wrote that the only hadron states found so far are two quark mesons and three quark baryons and that no exotic tetraquark, pentaquark, hybrid meson-gluon or molecular meson states have been confirmed beyond doubt yet. However, there are several candidates in the light tetraquarks and hidden charm sectors, and Perlovsek studied with lattice QCD light tetraquarks that may be the experimentally observed σ and κ mesons.

The quark exchange reaction between adjacent pion tetraquark tetrahedrons in the fabric may be seen as hadron scattering reactions. The d and u quarks for example are exchanged between an electron and pion tetraquarks and the scattering reaction is symmetric since the products are the same as the reactants. Note that quark exchange reaction may flip the vacuum pion tetraquark tetrahedron chirality and break the QCD vacuum chiral symmetry.

$$\tilde{u}d\tilde{d}u (\pi^{Td})_i + \tilde{u}d\tilde{d}u (\pi^{Td})_j \rightarrow \tilde{u}u\tilde{d}d (\pi^{Td})_i + \tilde{u}d\tilde{d}u (\pi^{Td})_j \quad (18)$$

Equation 9 above (on page 16) describes a two tetraquarks scattering reaction where the electron tetraquark is transformed to a pion tetraquark and vice versa. The tetraquark scattering reactions of equations 7, 9, 10, 17 and 18 may be studied with lattice QCD³⁵⁻³⁷. Few-body methods and constituent quark models³⁸ may also be used to calculate the binding energies of the proposed electron and pion tetraquarks.

9. Summary

We assume that the answers to the three questions raised in section 2 are positive and consider them as axioms of the quark model of the electron and the vacuum pion tetrahedron

fabric. Accordingly, the electron is not an elementary point like particle and not a single particle. The electron tetraquark tetrahedron forms with the vacuum pion tetraquark tetrahedrons fabric an electron cloud. The quantum vacuum has a structure formed by pion tetraquark tetrahedrons fabric with varying density. The pion tetraquark tetrahedron particles are made of 50% matter and 50% antimatter and hence the vacuum fabric is not made of ordinary particles. The electron motion occurs via u and d quark exchanges by tunneling through a potential barrier between electron tetraquark tetrahedrons and pion tetraquark tetrahedrons, and the exchanges of \tilde{u} and \tilde{d} antiquark flavors in the second electron tetraquark state. Some conclusions that may be derived from the proposed quark model for the electron and the vacuum fabric are: (a) Quark number and flavor are conserved quantities in the quark exchange reactions like the conservation of atoms and electrons in molecular reactions; (b) Quark exchanges may break the QCD vacuum state symmetry by flipping the chirality of the pion tetraquark tetrahedron enantiomers; and (c) Lattice QCD may prove the quark model for the electron and the vacuum pion tetrahedron fabric and may allow calculating the mass of the proposed pion and electron exotic tetraquarks.

References

- [1] Helge, K., (2009), “Wave Packets, Compendium of Quantum Physics, Concepts, Experiments, History and Philosophy.”, 828–830, Springer.
- [2] C. G. Darwin, (1927), "Free motion in the wave mechanics", Proceedings of the Royal Society of London. <https://royalsocietypublishing.org/doi/10.1098/rspa.1927.0179>
- [3] P. A. M. Dirac, (1928), “The Quantum Theory of the Electron”, https://www.physics.rutgers.edu/grad/601/QM502_2019/Dirac.pdf
- [4] Kaplan, I. G., (2019). ”Pauli Exclusion Principle and its theoretical foundation”, <https://arxiv.org/pdf/1902.00499>
- [5] Barut, A.O. and Pavsic, M., (1993), “Dirac's shell model of the electron and the general theory of moving relativistic charged membranes”, <https://www.sciencedirect.com/science/article/abs/pii/037026939391136B>

- [6] Feynman, R., “The Feynman Lectures on Physics, Quantum Mechanics”, https://www.feynmanlectures.caltech.edu/III_toc.html
- [7] Feynman, R. and Weinberg, S., (1987), “The Reason for antiparticles” https://www.cambridge.org/core/services/aop-cambridge-core/content/view/9D72E7C9045A9C0797DD952678F03C75/9781107590076c1_p1-60_CBO.pdf/the-reason-for-antiparticles.pdf
- [8] P. A. M. Dirac, (1928), “Lecture on the Foundation of Quantum Mechanics”, <https://mediatheque.lindau-nobel.org/recordings/34222/1965-the-foundations-of-quantum-mechanics>
- [9] Rom, R., (Apr 2023), “The Quantum Chromodynamics Gas Density Drop and the General Theory of Relativity Ether”, Journal of High Energy Physics, Gravitation and Cosmology, 9, No. 2. <https://www.scirp.org/journal/paperinformation.aspx?paperid=124153>
- [10] Rom, R., (Apr 2023), “Matter Reactors”, Journal of High Energy Physics, Gravitation and Cosmology, 9, No. 2. <https://www.scirp.org/journal/paperinformation.aspx?paperid=124154>
- [11] Rom, R., (Apr, 2024), “Non-Uniform Pion Tetrahedron Aether and Electron Tetrahedron Model”, Journal of High Energy Physics, Gravitation and Cosmology. <https://www.scirp.org/journal/paperinformation?paperid=132602>
- [12] Rom, R., (Jan 2024), “The Pionic Deuterium and the Pion Tetrahedron Vacuum Polarization”, Journal of High Energy Physics, Gravitation and Cosmology, 10, No. 1. <https://www.scirp.org/journal/paperinformation?paperid=130928>
- [13] Rom, R., (May 2024), “QCD’s Low Energy Footprint”, <https://vixra.org/abs/2403.0128>
- [14] Peters, A., (2014), “Determination of $\Lambda_{\overline{MS}}$ from the static quark-antiquark potential in momentum space”, Master thesis. https://itp.uni-frankfurt.de/~mwagner/theses/MA_Peters.pdf
- [15] Lee, T., (2012), “Vacuum quark condensate, chiral Lagrangian, and Bose-Einstein statistics”, <https://arxiv.org/abs/1206.1637>
- [16] Brodsky, S. B., Shrock, R., (2008), “On Condensates in Strongly Coupled Gauge Theories”, <https://arxiv.org/abs/0803.2541>
- [17] Brodsky, S. B., Roberts, C. D., Shrock, R., Tandy, P.C., (2010), “Essence of the vacuum quark condensate”, <https://arxiv.org/abs/1005.4610>
- [18] Buballa, M., Carignano, S., (2014), “Inhomogeneous chiral condensates”, <https://arxiv.org/abs/1406.1367>
- [19] Byers, N., (1998), “E. Noether’s Discovery of the Deep Connection Between Symmetries and Conservation Laws”, <https://arxiv.org/abs/physics/9807044>

- [20] Burkert, V.D. et al, (2022), “Precision Studies of QCD in the Low Energy Domain of the EIC”,
https://www.researchgate.net/publication/365850432_Precision_Studies_of_QCD_in_the_Low_Energy_Domain_of_the_EIC
- [21] Paraoanu, G.S., (2014), ”The Quantum Vacuum”, <https://arxiv.org/abs/1402.1087>
- [22] Keenan, R.C., Barger, A.J, Cowie, L.L., (2013) “EVIDENCE FOR A ~ 300 MEGAPARSEC SCALE UNDER-DENSITY IN THE LOCAL GALAXY DISTRIBUTION”, The Astrophysical Journal, 775:62 (16pp), 2013, September 20.
- [23] Banik, I., (Nov 20, 2023), “Do we live in a giant void? It could solve the puzzle of the Universe’s expansion”, <https://theconversation.com/do-we-live-in-a-giant-void-it-could-solve-the-puzzle-of-the-universes-expansion-216687#:~:text=When%20we%20measure%20the%20expansion,area%20with%20below%20average%20density>).
- [24] Mazurenko, S., Banik, I., Kroupa, P., Haslbauer, M., (Nov 20, 2023), “A simultaneous solution to the Hubble tension and observed bulk flow within $250 h^{-1}$ Mpc”,
<https://arxiv.org/abs/2311.17988>
- [25] Grabovsky, D, (2021), “The Double Well”,
<https://web.physics.ucsb.edu/~davidgrabovsky/files-teaching/Double%20Well%20Solutions.pdf>
- [26] Pengra, D., (2023), “The Inversion Spectrum of Ammonia”,
https://courses.washington.edu/phys432/NH3/ammonia_inversion.pdf
- [27] Santos, I. U., (2023), “The zitterbewegung electron puzzle”,
https://www.researchgate.net/publication/374257062_The_zitterbewegung_electron_puzzle
- [28] Davis, B.S., (2020), “Zitterbewegung and the Charge of an Electron”,
<https://arxiv.org/abs/2006.16003>
- [29] Hui, D., Alqattan, H., Sennary, M., Golubev, N., Hassan, M., (2024), “Attosecond electron microscopy and diffraction”, <https://www.science.org/doi/10.1126/sciadv.adp5805>
- [30] t-Hooft, G., (2004), “Renormalization without Infinities”
<https://arxiv.org/pdf/hep-th/0405032>
- [31] Bergere, M. C., and Zuber, J. Z., (1973), “Renormalization of Feynman Amplitudes and Parametric Integral Representation”
https://www.lpthe.jussieu.fr/~zuber/MesPapiers/bz_CMP74.pdf
- [32] Blechman, A. E., (2002), “Renormalization: Our Greatly Misunderstood Friend”,

<http://www.pha.jhu.edu/~blechman/papers/renormalization/renormalization.pdf>

[33] Ukawa, A., (2015), “Kenneth Wilson and lattice QCD”,
<https://arxiv.org/abs/1501.04215>

[34] Boyle, P. et al, (2022), “Lattice QCD and the Computational Frontier”,
<https://arxiv.org/abs/2204.00039>

[35] Prelovsek, S. et al, (2010), “Lattice study of light scalar tetraquarks with $I = 0, 2, 1/2, 3/2$: are σ and κ tetraquarks?”, <https://arxiv.org/abs/1005.0948>

[36] Ortiz-Pacheco, E. et al, (2023), “Doubly charmed tetraquark: isospin channels and diquark-antidiquark interpolators”, <https://arxiv.org/abs/2312.13441>

[37] Alexandrou, C., Berlin, J., Finkenrath, J., Leontiou, T., Wagner, M., (2019), “Tetraquark interpolating fields in a lattice QCD investigation of the $D_{s0}^*(2317)$ meson”,
<https://arxiv.org/abs/1911.08435>

[38] Meng, L., Chen, Y., Ma, Y., Zhu, S., (2023), “Tetraquark bound states in constituent quark models: benchmark test calculations”, <https://arxiv.org/abs/2310.13354>